High Frequency Performance of Multilayer Capacitors

Arthur T. Murphy, *Fellow, IEEE*, and Frederick J. Young

***Abstract*—The high frequency performance of capacitors is related to their geometry and material properties. By considering multilayer capacitors (MLC) as distributed electrical systems, computer-aided multi-conductor transmission line analyses is applied to study resonant frequencies, equivalent circuits of capacitors, and the influence of ground planes, test fixtures, and type of connection topology. The methods established are applied to well-documented capacitors described in the literature and good agreement between experimental results and analyses is obtained.**

I. Introduction

At VERY low frequencies, capacitors exhibit ideal behavior and have only three properties. These are the capacitance, dissipation factor, and voltage rating. Under such circumstances it does not matter how the external circuit is connected to the capacitor plates and the presence of other conductors is unimportant. As the frequency rises, each lead and every current path inside the capacitor has an increasing inductive effect and eventually becomes a transmission line of sorts. Then capacitors show resonances and antiresonances which may be influenced by the lead placement or the presence of ground planes. Although high frequency phenomena in capacitors have been described before [4], [5], and [11] they have not been analyzed using the recent advances in the calculation of electromagnetic fields. These new methods allow an exact treatment of distributed multilayer structures [12], [13]. It is our goal to examine some high frequency phenomena from a fundamental view point utilizing the distributed analyses of ICONSIM [1] (computer aided interconnection simulation) and appropriate physical models of capacitors. In all cases the parameters of the physical models of the capacitors are derived from the capacitor geometry and the physical properties of the materials used.

II. Summary of the Results of New Methods

A. General Purpose

It is our goal to verify our new methods of capacitor analyses with experimental results given in the literature. Although many papers present experimental results for various types of capacitors, very few give sufficient detail about the geometry and material properties to enable an analysis based upon physical principles. Our new methods are applied to capacitors measured by Boser and Newsome [2] and Burn and Porter [3] which have 2 and 6 plates, respectively.

Manuscript received October 14, 1992; revised May 25, 1995.

A. T. Murphy is with Central Research and Development, Experimental Station, E. I. du Pont de Nemours & Co. Inc., Wilmington, DE 19880-0174 USA.

F. J. Young is at 800 Minard Run Road, Bradford, PA 16701-3718 USA.

IEEE Log Number 9413416.

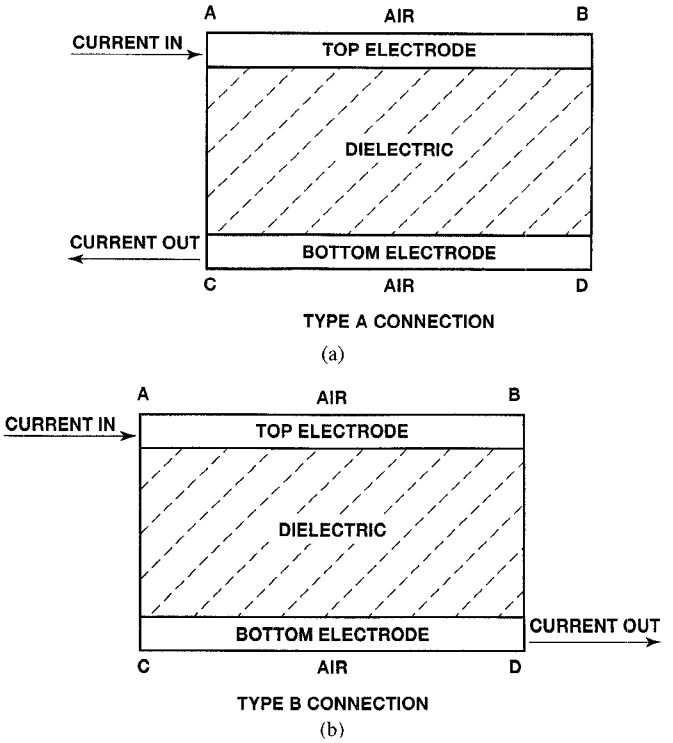

Fig. 1. Capacitor connection topology.

B. Important New Conclusions

1) The Influence of Connection Topology: In a two electrode capacitor the leads may be attached at any point on the plate as long as each plate has but one lead connected to it. At dc and low frequencies all such connections made at arbitrary locations on the plates yield the same value of capacitance. At higher frequencies, when electrode inductance and resistance become important, the exact nature of the connections must be considered. In this work we consider the two simplest connections. In a type A connection current enters and leaves on the same side of the capacitor, while in a type B connection current enters and leaves on opposite sides. Fig. 1 shows both type A and type B connections.

We show that type A topology leads to a high resonant frequency and high equivalent series resistance (ESR). The type B connection yields a low resonant frequency and a low

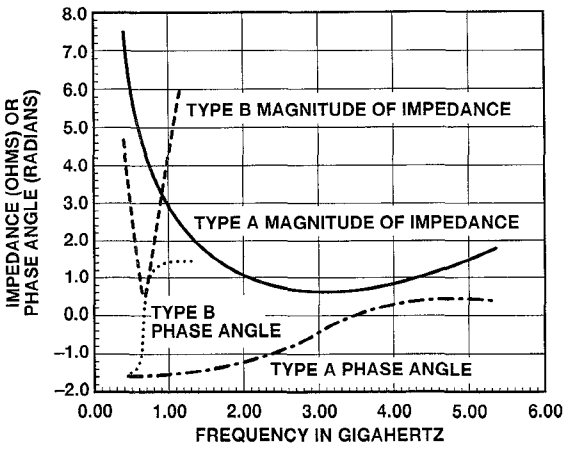

Fig. 2. Calculated impedance and phase angle—comparison of type A and type B connections for the Boser and Newsome [2] NPO2S1 capacitor.

ESR. This is illustrated in Fig. 2 which shows our calculated impedance versus frequency curves of one of Boser and Newsome's [2] capacitors for type A and B topologies. In the type A connection the resistive losses cause the minimum in the magnitude of the impedance to occur at 3.05 gigahertz instead of 3.45 gigahertz where the phase angle is zero and the impedance is a pure resistance of 620 milliohms. In a type B connection the minimum magnitude of the impedance occurs at 0.639 gigahertz whilst the phase angle is zero at 0.640 gigahertz where the impedance is a pure resistance of 520 milliohms. Note the great difference between resonant frequencies indicating that a type A connected capacitor acts as a capacitor over a much greater frequency range than does a type B connected capacitor. The resistance for a type A topology is about 16% larger than for type B in this case.

2) The Influence of Ground Planes and Test Fixtures: Each electrode of a capacitor has a self inductance that is reduced progressively as ground planes or ground conductors are moved closer. The mutual coupling is not changed as greatly and capacitance is not influenced. The resistances are also influenced by ground conductors. It is well known in the measurement of type B connected capacitors that the test fixture exerts an influence on the measured resonant frequency. This is because part of the test fixture is a pipe-like ground which causes the capacitor electrode inductance to vary as a function of its internal diameter.

We have obtained additional information [6] pertaining to the capacitors of Boser and Newsome [2] of Philips Laboratories at Briarcliff, NY. The two plate NP02S1 capacitor depicted in Fig. 3 is analysed.

In this capacitor, utilizing a type B connection, current enters at side A of the top conductor and leaves at side B of the bottom conductor. Boser and Newsome [2] measured a resistance of 520 milliohms at the first resonant frequency of 660.6 megahertz and a capacitance of 50 picofarads. Our mathematical models based upon the physical properties of the materials and the geometry yield 525 milliohms resistance at a resonant frequency of 639 megahertz. Our calculations in agreement with the original capacitor design indicate that dielectric losses are not important at this frequency. If the conductors are assumed to be lossless the calculated resonant

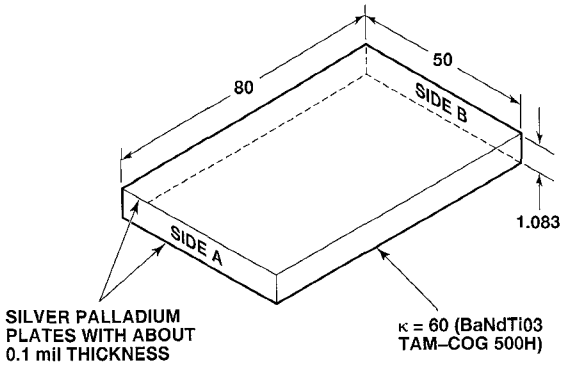

Fig. 3. Boser and Newsome's [2] two plate capacitor geometry with all dimensions in mils.

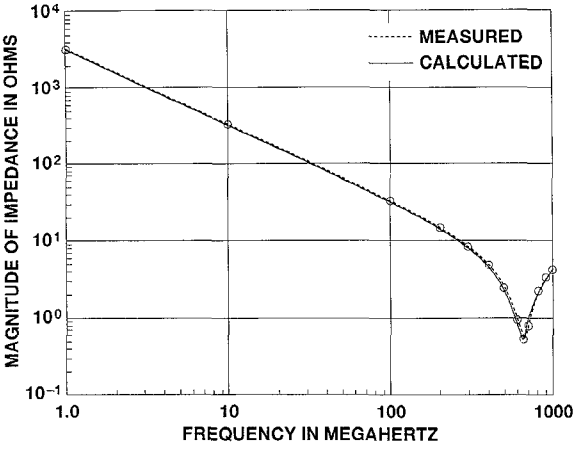

Fig. 4. Comparison of measured and calculated impedance of the NPO2S1 capacitor of Boser and Newsome [2].

frequency is 676 megahertz. In Fig. 4 is a comparison of our calculated and the measured impedance. The details of these calculations are given in Section III-A. Boser and Newsome [2] also measured an "identical" capacitor which they called NPO2S2. It had the same resonant frequency but only 310 milliohms of resistance.

C. Six-Plate Multilayer Capacitor

Capacitors are often constructed with several layers of dielectric separated by thin conducting layers which serve as the capacitor plates. In Fig. 5 is shown a multilayer capacitor (MLC) constructed and tested by Burn and Porter [3]. For simplicity, we show the capacitor electrodes or plates to be of zero thickness.

The area of the top of each dielectric layer is the overlap area and sets the value of capacitance. Using a value of 18.5 for the relative permittivity of the layers yields a total dc capacitance of 100 picofarad. The influence of the test fixture in which the MLC is mounted must be considered. The presence of a ground structure can greatly alter the inductance of the capacitor plates. The closer the ground structure, the lower said inductance is. In Fig. 6 is shown the MLC in the 1 centimeter ID test fixture. Measurements indicate Burn and Porter's [3] MLC Test Fixture introduces about 0.5 nanohenry of lead inductance which is included in our calculation of impedance as a function of frequency. We calculate a first resonant

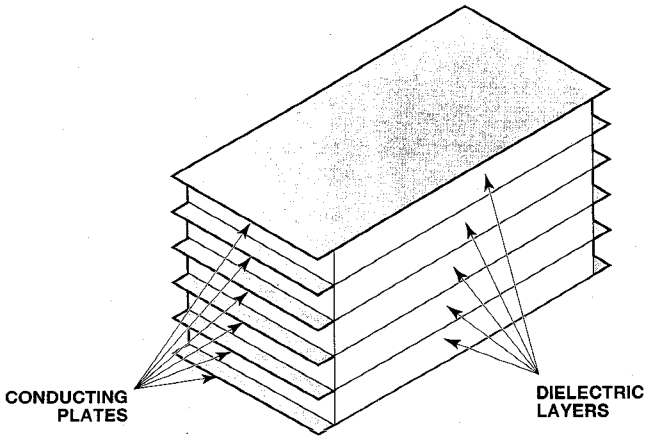

Fig. 5. The MLC geometry.

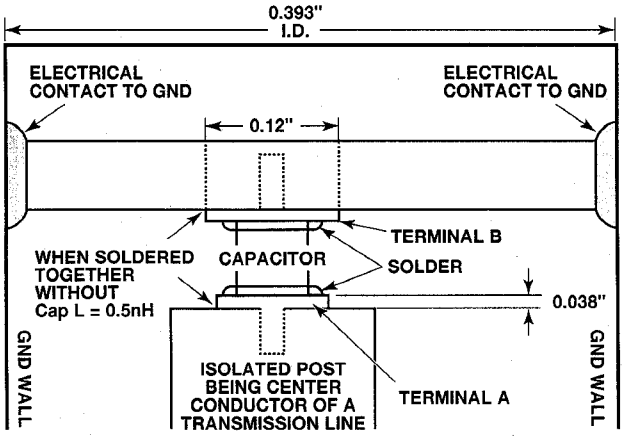

Fig. 6. Geometry of the MLC in the Burn and Porter's [3] test fixture.

frequency of 372 megahertz and estimate an impedance of about 20 milliohms at that frequency. The experimental results using this test fixture and the HP8510B network analyzer yield 19.96 milliohms at a frequency of 379 megahertz.

The same capacitor was tested in a 0.275" ID coaxial test fixture. The measured resonant frequency was 424 megahertz and lead inductance was thought to be 0.368 nanohenry. Using that value of lead inductance our calculations predict a resonant frequency of 387 megahertz. Had we used a lead inductance of 0.25 nanohenry we would have predicted a resonant frequency of 424 megahertz, also.

III. The Modeling of Capacitors

A. Simple Parallel Plate Capacitor

If a simple parallel plate capacitor illustrated in Fig. 7 is to be modeled, it may at first seem that there is no doubt about the proper model. All that is needed are good connections to the top and bottom plates at any location. Assuming very low frequency and ideally conducting plates, these connections would hold each plate at the desired uniform potential. As the frequency increases the conductors and dielectrics become lossy and the inductance of the current paths becomes important. Then the exact nature of the connection of capacitor leads becomes important.

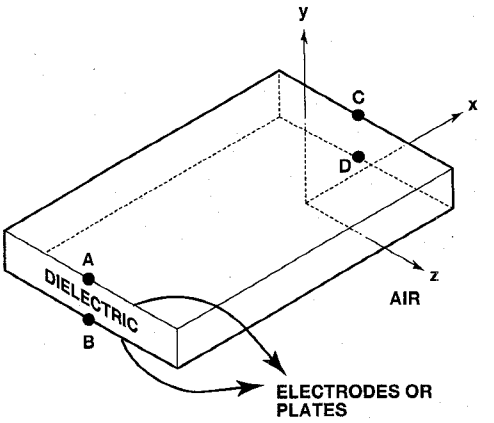

Fig. 7. Simple parallel electrode capacitor.

Although there are infinitely many ways to attach leads to capacitor plates, we shall consider only two which are commonly used. If the voltage source is connected to points A and B such that current enters point A and exits point B or vice versa, the capacitor acts as an open circuited transmission line with propagation in the x direction. This is the way people tend to view capacitors and it shall be called a type A connection. For the point connections shown there will also be propagation in the z direction near points A and B. We shall not worry about that because electrodes spanning the z width of the capacitor can be used to hold the potential constant along the edges of the top and bottom plates thereby eliminating propagation in the z direction. In this case the appropriate radio frequency model is an ordinary transmission line. The capacitance, inductance and resistance for the model can be easily determined by use of ICONSIM [1]. In addition, a lumped equivalent series R, L, C circuit is easily derived for a low frequency model of the simple parallel plate capacitor. Such a model can provide accurate results only below the first resonant frequency of the capacitor where the impedance seen between points A and B is minimal and purely reactive.

Even the simple two plate capacitor may not be connected always in the aforementioned way. Current could enter at point A and exit point D. Such a connection is denoted by type B (see Fig. 1). Some thick film planar filter connectors and microwave coupling capacitors are connected this way.

It is clear that a simple parallel plate capacitor no longer acts as a single transmission line, but becomes a coupled two conductor transmission line. The top and bottom plates are the coupled conductors which interact in even and odd modes above the ground.

The omnipresence of the ground, however remote, is the key to modeling capacitors in the radio frequency range. It provides us with the notion that even a simple parallel plate capacitor is a two conductor coupled transmission line. Knowing that, we can use ICONSIM [1] tools to calculate the requisite matrices for a CW or transient analysis based upon the theory of coupled transmission lines [9].

B. Equivalent Circuits

The equivalent circuits are derived from the inductance $[L]$, electrostatic induction coefficient $[K]$, resistance $[R]$,

and conductance $[G]$ matrices of the capacitor. The diagonal terms of the inductance coefficient matrix are the self inductances of the corresponding plates. The remainder of the coefficients represent mutual inductances between plates. The off-diagonal terms of the electrostatic induction coefficient matrices represent the negative of the capacitances between the corresponding plates. The capacitances between each plate and ground are given by summing the rows of the electrostatic induction coefficient matrix. These matrices must be calculated from the capacitor geometry and require the presence of a ground or reference conductor in addition to the capacitor plates. If the reference conductor is located at a distance much greater than the plate dimensions it does not affect the resistance and inductance matrices. However, in many applications and tests the reference conductor is close enough that it influences the R and L matrices. Because the material between the plates has a relative permittivity much greater than that of air, the C and G matrices are not related to the location of the reference conductor.

1) Current Entering and Leaving on the Same Side (Type A): When current enters the plate at the edge containing point A and leaves at the edge containing point B in Fig. 7, the capacitor behaves as an ordinary two conductor transmission line. This characterization of a capacitor is old and is the one most engineers are prone to use, even when not applicable. It is not applicable in any case where the current does not enter and exit at opposing points on the plates or on the same side of the capacitor. The ordinary transmission line parameters can be obtained from the aforementioned matrices. They are given by

$$L = L_{11} + L_{22} - 2L_{12} \tag{1}$$

$$C = -K_{12} \tag{2}$$

$$R = R_{11} + R_{22} + 2R_{12} \tag{3}$$

$$G = -G_{12}. \tag{4}$$

In the expression for total inductance (1) the mutual term subtracts because the currents in the two plates of the capacitor flow in opposite directions. In the circuit of the top plate current flowing in the top plate causes an inductive voltage drop whereas current flowing the opposite direction in the bottom plate causes an inductive voltage rise. All electrode currents, dielectric displacement currents, and ground plane currents form a closed loop in which a magnetic field is generated. An alternating current in the top electrode and ground loop produces a time-varying magnetic field, a field which induces a current in the bottom electrode. The induced current in the bottom electrode increases as a function of frequency and tends to be in the opposite direction to the current in the top electrode. These induced currents cause mutual resistance which is zero at zero frequency. The mutual resistances comprise the off-diagonal terms in the resistance matrix. The diagonal terms are the ac resistances of each individual electrode. At zero frequency they are the dc electrode resistances and they increase as frequency increases. Although the mutual resistance is due to induced currents it does not behave the same way as mutual inductance. Due to the proximity effect resistance, increases in cases where the currents flow in opposite directions. Thus in (3) the mutual resistance adds to the total capacitor resistance. The impedance seen looking into the terminals of such a lossy transmission line depends on how it is loaded. In the case of a capacitor with the source connected between terminals A and B the load connected between terminals D and C (see Fig. 7) is infinite. Then the impedance seen between terminal A and B is given

$$Z_{in} = Z_0 \coth \gamma \ell \tag{5}$$

where $\gamma = [(R + j\omega L)(G + j\omega C)]^{0.5}$ and $Z_0 = [(R + j\omega L)/(G + j\omega C)]^{0.5}$. When the losses are neglected (5) becomes

$$Z_{in} = -jZ_0 \cot \beta \ell \tag{6}$$

where $\beta = \omega\sqrt{LC}$ and $Z_0 = \sqrt{L/C}$. Here Z_0 is the characteristic impedance of the line in ohms, L, C, G, and R are the unit length values of inductance, capacitance, conductance and resistance. Here ℓ is the line length. Any consistent set of units may be used for these quantities. The input impedance given by (5) for the general lossy case is not simple and is most easily examined numerically for each particular case. When the losses are very low (6) is useful and discloses the presence of resonances where the impedance becomes zero and antiresonances where the impedance becomes infinite. When $\cot(\omega\ell)\sqrt{LC})$ equals zero the series resonances characterized by zero input impedance occur. Then

$$f_{is} = i/(4\ell\sqrt{LC}/) \tag{7}$$

where $i = 1, 3, 5 \ldots$. Parallel resonances occur when $\tan \omega\ell\sqrt{LC} = 0$. Then

$$f_{ip} = i/(2\ell\sqrt{LC} \tag{8}$$

where $i = 1, 2, 3 \ldots$. To obtain a lumped equivalent circuit for the transmission line we use the power series expression for $\coth x = 1/x + x/3 - x^3/45 + \cdots$. Then (5) becomes

$$Z_{in} \approx [(G + j\omega C)\ell]^{-1} + (R + j\omega L)\ell/3 \tag{9}$$

which is the impedance of the lumped equivalent circuit given in Fig. 8. Here L_{11} must equal L_{22} in order for the ordinary transmission line theory to apply. Here we note the equivalent circuit of a capacitor is not the simple series R, L, C circuit so often mentioned in the literature, except when $G = 0$. It is easy to show from (9) that the equivalent series impedance, (ESZ) is given by

$$\begin{aligned} \mathrm{ESZ} = {} & R\ell/3 + 1/[(1 + \omega^2 C^2/G^2)G\ell] \\ & + j/(\omega L\ell/3 - 1/[(1 + G^2\omega^2/C^2)\omega C\ell]) \end{aligned} \tag{10}$$

which becomes real when

$$f = \frac{1}{2\pi}\sqrt{\frac{3}{LCl^2} - \frac{G^2}{C^2}} \tag{11}$$

and

$$\mathrm{ESZ} = \mathrm{ESR} = Rl/3 + GLl/3C \tag{12}$$

where ESR is the equivalent series resistance. This expression can be used as a criterion for assessing the importance of

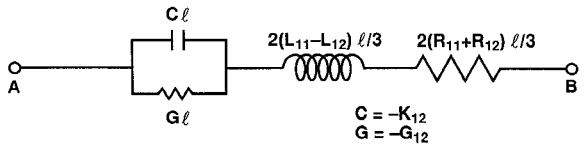

Fig. 8. The lumped equivalent circuit of a two plate capacitor when current enters and leaves on the same side of the plates (type A). See Fig. 7 for corresponding terminal labels.

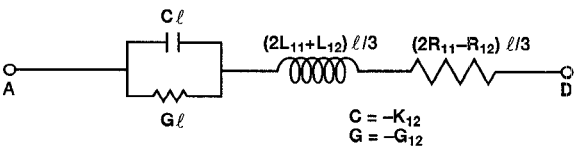

Fig. 9. The lumped equivalent circuit for a capacitor in which current enters and leaves on opposite sides (type B). See Fig. 7 for corresponding terminal labels.

dielectric losses with respect to conductor losses. They are negligible if

$$G \ll RC/L. \tag{13}$$

It is clear that as plate resistance diminishes dielectric losses assume more importance and as inductance decreases dielectric losses become less in comparison to resistive losses.

2) Current Entering and Leaving on Opposite Sides (Type B): In Fig. 7 current might enter on the side where terminal A is located and exit the other side at terminal D. For two plate capacitors it is possible to make either this or the previous connection. However, when more than two plates are used the current usually enters and exits on opposite sides. As frequency increases such a configuration requires a transmission line type analysis. However, this is not a conventional transmission line because current enters and exits on opposite sides. In the Appendix an analysis of such a configuration is presented. The impedance of this capacitor configuration is given by (14) shown at the bottom of the page, where $Z_T = R_{11} + j\omega L_{11}$, $Z_B = R_{22} + j\omega L_{22}$, $Z_M = -R_{12} + j\omega L_{12}$, $\alpha = \sqrt{Y(Z_T + Z_B - 2Z_M)}$, $Y = -(G_{12} + j\omega K_{12})$ and ℓ = the mean length of the capacitor plates. Here the sign on the real part of Z_M is negative because the currents in both plates flow in the same direction. Current flow in the bottom plate tends to induce current flow in the opposite direction in the top plate thereby reducing the power loss. It is not easy to find a simple equivalent circuit which has approximately the same impedance as (14). When both plates of the capacitor are the same or when $Z_T = Z_B = Z$ (14) becomes

$$Z_{in}=[(Z+Z_M)\alpha\ell+2(Z - Z_M)(1+\cosh\alpha\ell)]/(2\alpha\sinh\alpha\ell). \tag{15}$$

The first two terms of the Taylor series representation of (15) yield

$$Z_{in} = \frac{1}{(G + j\omega C)\ell} + (2Z + Z_M)\ell/3 \tag{16}$$

whence the equivalent circuit is given in Fig. 9. The comparison of (9) and (16) or Figs. 8 and 9 indicates that the method of connecting to a capacitor greatly influences its inductance and resistance. Equivalent series impedance, (ESZ) is given by

$$\mathrm{ESZ} = R_B\ell/3 + 1/[(1 + \omega^2C^2/G^2)G\ell] + j\{\omega L_B\ell/3 - 1/[(1 + G^2\omega^2/C^2)\omega C\ell]\} \tag{17}$$

which becomes real when

$$f = \frac{1}{2\pi}\sqrt{\frac{3}{L_BC\ell^2} - \frac{G^2}{C^2}} \tag{18}$$

and

$$\mathrm{ESZ} = \mathrm{ESR} = R_B\ell/3 + GL_B\ell/(3C) \tag{19}$$

where the L_B and R_B are defined as

$$L_B = 2L_{11} + L_{12} \tag{20a}$$

$$R_B = 2R_{11} - R_{12}. \tag{20b}$$

C. Two Plate Capacitor Observations and Conclusions

The comparison of the equivalent circuits of the two kinds of two plate capacitor connections is very important. Each connection has its advantage. The first case where currents exit and enter on the same side of the plates has less inductance and more resistance due to the conductors than does the case where currents enter and exit on opposite sides. The difference between the two connections in inductance and resistance is about $3L_{12}$ and $3R_{12}$. For closely coupled plates this represents a large percent of change. Thus, the ordinary capacitor connection yields a high resonant frequency at the expense of a high ESR and the connection where current enters and exits on opposite sides suffers from a much lower resonant frequency with the dividend of a lower ESR. These conclusions hold provided the dielectric losses are not nearly as large as the ohmic losses. When the dielectric losses predominate there seems nothing to be gained from the use of the less common connection.

D. Multilayer Capacitors (MLC)

It would be possible to derive a new transmission line theory for capacitors having more than two plates, just as we have done for the two plate capacitors. Such a distributed theory would result in very cumbersome mathematical results and complicated equivalent circuits. Instead we shall use coupled transmission line equivalent circuits which are very simple

$$Z_{in} = \left\{\frac{[(Z_BZ_T - Z_M^2)\alpha\ell+(Z_B-Z_M)(Z_M-Z_T)\sinh\alpha\ell]\sinh\alpha\ell-[(Z_M-Z_T)\cosh\alpha\ell-Z_B+Z_M][(Z_B-Z_M)\cosh\alpha\ell+2Z_T-Z_B-Z_M]}{(Z_B-2Z_M+Z_T)\alpha\sinh\alpha\ell}\right\} \tag{14}$$

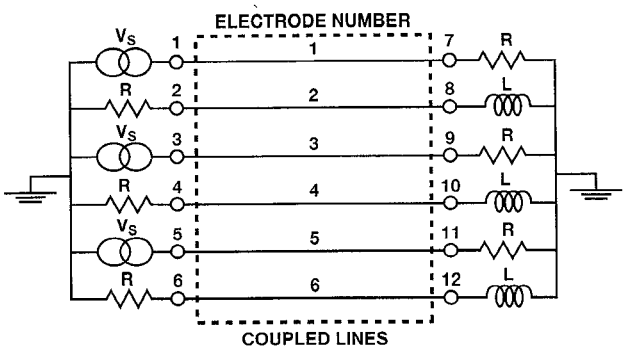

Fig. 10. Edge view of an MLC showing terminations.

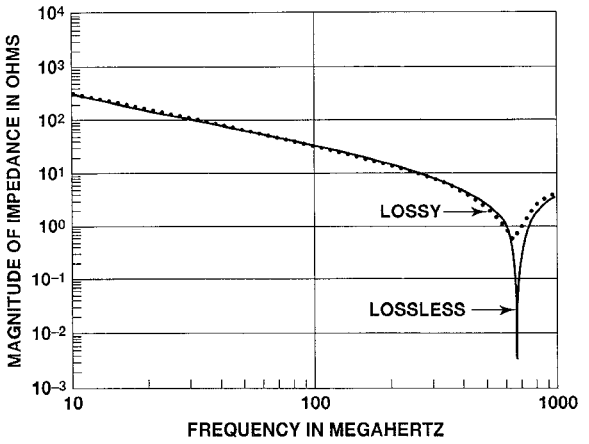

Fig. 11. Comparison of lossy and lossless impedance calculation for the Boser and Newsome [2] MPO2S1 capacitor.

and can be analysed by various parts of ICONSIM [1]. Fig. 10 shows an edge view of an MLC with six plates. Here we note electrodes 1, 3, and 5 are excited by a voltage source V_s at terminals 1, 3, and 5. Plates 2, 4, and 6 are open circuited on the excited end of the capacitor. On the other end of the capacitor electrodes 1, 3, and 5 are open circuited and electrodes 2, 4, and 6 are loaded with the lead or test fixture inductance, L. The open circuits are simulated by making $R = 10^8$ ohms. To make an analysis of an MLC we treat the assemblage of capacitor plates as a multiconductor transmission line. Various ICONSIM [1] programs are available to analyse such configurations.

IV. Details of the Treatment of Practical Capacitors

In this section we describe in detail how the analyses of these capacitors are performed.

A. Boser and Newsome's [2] Capacitor

After reading Boser and Newsome's paper [2] we requested more information and obtained their internal report [7]. It contained details pertaining to their capacitors, their geometry and measurement. According to Boser [6] the capacitor electrodes are about 0.1 mil thick and are rather porous so that the effective conductivity of them is considerably less than that of silver palladium. To obtain the measured value of resistance at the resonant frequency we adjusted the electrical conductivity to 1.2×10^6 s/m. Such a low conductivity is expected in silver palladium conductors because of voids and impurities. Poulin [8] has worked with silver palladium conductors with electrical conductivity of 2×10^6 s/m. The calculation of the matrices was done at 640 megahertz by the programs of ICONSIM [1] which use boundary element methods.

Using a dissipation factor of 0.002 (a nominal book value for the dielectric) the matrices, given in detail in an earlier conference paper [12] were obtained. By solving the coupled transmission line equations in the frequency domain allowing for frequency variation in the matrices we obtain the calculated curve given in Fig. 4 which exhibits 0.52 ohms impedance at a frequency of 639 megahertz. It is of interest to note constant downward slope of the impedance which changes only above a frequency of 200 megahertz. Thus, below that frequency it behaves as a constant, slightly lossy capacitor. In Fig. 11 is a comparison of these results to lossless results. Here we see the resonant frequency shift up to 676 megahertz when no losses are present. We checked our results by the methods of Matsushita and Moto-Oka [9] and the equivalent circuit of Section II-B-2 shown in Fig. 9. Both yield a resonant frequency of 676 megahertz and a resistance at resonance of 450 milliohms. Calculations with $G = 0$ yielded identical results and we conclude dielectric losses are not important at the frequencies considered here. Boser and Newsome's [2] measurements indicate a dissipation factor of zero at 1 kilohertz. It seems that the electrode microstructure must be studied carefully so that its effective conductivity is well known. At present one cannot really determine the R matrix solely from nominal geometry and material properties.

B. The Six-Electrode Capacitor of Burn and Porter [3]

Burn and Porter [3] had experimental data on their six electrode MLC. The geometry is shown in Fig. 5. The location of the ground plane greatly influences the inductance matrix. The MLC was tested in the test fixture shown in Fig. 6. Here the MLC is mounted in a 393 mil (9.98 mm) cylinder and connected with slightly inductive terminals A and B. The use of ICONSIM assuming a lossless dielectric produced the matrices given in detail elsewhere [12]. We use the circuit of Fig. 10. Measurements indicate the MLC Test Fixture introduces about 0.5 nanohenry of lead inductance. This value can also be obtained by an inductance calculation based upon the Test Fixture geometry. Thus, we let L in Fig. 10 be 1.5 nanohenry. The three parallel inductances then amount to the inductance of the MLC test fixture. The plot of the magnitude of impedance seen by the source as a function of frequency is given in Fig. 12. The first resonant frequency occurs at 372 megahertz. The measured first resonant frequency was found to be 380 megahertz by Porter [10]. Our calculations indicate anti or parallel resonances at 0.818 and 6.7587 gigahertz and additional series resonances at 0.83 and 6.7593 gigahertz. These calculations assume no electrode losses. The inclusion of losses, with $[R]$ proportional to the square root of frequency almost eliminates the higher frequency resonances. In order to make a more exact calculation with losses we calculated the R matrix at 0.372 gigahertz. The inclusion of conductor losses does not alter the first resonant frequency. The resistance

matrix is not of the highest quality because it contains some negative numbers. They were made positive and several times larger with no influence upon the resulting impedance. These numbers are in the "noise level" of the numerical process.

It is notable that the dimensions of the test fixture can significantly affect the resonant frequency. For example, reducing the test fixture ID from 0.393 inches to 0.274 inches raises the resonant frequency from 380 to 424 megahertz and reduces resistance at resonance from 84 to 79 milliohms.

V. Conclusion

We have demonstrated that single and multilayer capacitors can be accurately modeled as multi-conductor transmission lines using modern computer-aided analyses. We are able to predict the resonant frequencies and impedance variation with frequency from basic geometry and material properties. These have been compared to experimental results given in the literature with excellent agreement (Fig. 4). Equivalent circuits have been derived from analytical expressions resulting from transmission line analyses (Figs. 8 and 9). Here is presented one of the first studies of the mutual resistance of conductors which shows how they are used in circuit analysis.

We have also shown that two basically different lead attachment connections result in radically different high frequency performance (Fig. 2). If the connection current enters and leaves on the same side of the capacitor (Type A), it will display a high resonant frequency and a high ESR. If the current enters and leaves on opposite sides (Type B), it will display a lower resonant frequency and a lower ESR.

Appendix
Analytical Solution for Type B Connection

Here an analytical solution is obtained for a two plate capacitor in the type B connection. In contrast to an analysis by Coda and Selvaggi [5] we account fully for the mutual inductances and resistances and their variation with frequency. The results agree with a numerical simulation and allow some insight into the effect of various parameters.

As pointed out earlier the high dielectric permittivity region of capacitors behave as transmission lines. However, when used with a type B connection they cannot be considered to be ordinary transmission lines because of the direction of current flow. In an ordinary transmission line current flows into terminal A and back out of terminal B (see Fig. 1). In this capacitor with a type B connection current flows into terminal A, none flows at terminals B and C and the current flows out of terminal D. The total conduction current in the top plate is conveyed to the bottom plate via displacement current in the dielectric. Such a phenomena is represented by a cascade of the impedances as shown in Fig. 13. Here $R_{11}, R_{22}, L_{11}, L_{22}, L_{12}, R_{12}$, and Y are resistance, inductance, mutual inductance, mutual resistance, and admittance per unit length, T and B are top and bottom voltages, respectively. When the number of elements in cascade is taken to infinity there results

$$-\frac{dT}{dx} = Z_T i^T + (Z_M) i^B \tag{A1}$$

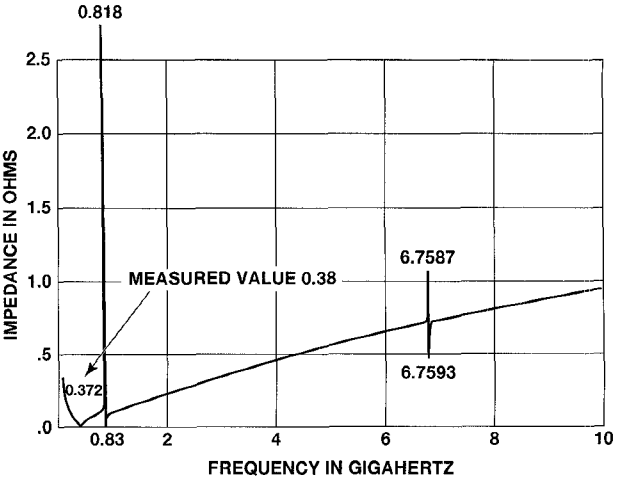

Fig. 12. Magnitude of impedance seen at the near end of an MLC.

$$-\frac{dB}{dx} = Z_B i^B + (Z_M) i^T \tag{A2}$$

$$-\frac{di^T}{dx} = Y(T - B) \tag{A3}$$

$$i_0 = i^T + i^B \tag{A4}$$

where $Z_T = R_{11} + j\omega L_{11}$, $Z_B = R_{22} + j\omega L_{22}$, $Y = G + j\omega C$, $Z_M = -R_{12} + j\omega L_{12}$, i_0 is the total current and, i^T and i^B are the currents in the top and bottom conductors. These equations can be combined to yield

$$\frac{d^2 i^T}{dx^2} - \alpha^2 i^T = -\frac{\alpha^2}{2} i_0. \tag{A5}$$

The solution to (A5) is

$$\begin{aligned} i^T = {} & \{(Z_B - Z_M) + (Z_T - Z_M)\cosh \alpha x \\ & + [Z_B - Z_M + (Z_T - Z_M)\cosh \alpha \ell] \\ & \times \sinh \alpha x / \sinh \alpha \ell\} i_0 / (Z_T - Z_B - 2Z_M) \end{aligned} \tag{A6}$$

whence

$$\begin{aligned} i^B = {} & \{(Z_T - Z_M)(1 - \cosh \alpha x) \\ & + [Z_B - Z_M + (Z_T - Z_M)\cosh \alpha l] \\ & \times (\sinh \alpha x) / \sinh \alpha \ell\} i_0 / (Z_T + Z_B - 2Z_M). \end{aligned} \tag{A7}$$

Here $i^T(x = 0) = i^B(x = \ell) = i_0$, $i^T(x = \ell) = i^B(x = 0) = 0$ and $\alpha = [Y(Z_T + Z_B - 2Z_M)]^{1/2}$. The voltage B is found by integrating (A2) using the results of (A5) and (A6). Here we assume $B(x = \ell) = 0$. Then

$$\begin{aligned} & B(x) \\ & = \{(Z_B Z_T - Z_M^2)(\ell - x) + [(Z_M - Z_B)(Z_T - Z_M)] \\ & \quad \times (\sinh \alpha \ell - \sinh \alpha x)/\alpha + (Z_B - Z_M) \\ & \quad \times [Z_B - Z_M + (Z_T - Z_M)\cosh \alpha \ell] \\ & \quad \times (\cosh \alpha \ell - \cosh \alpha x)/\alpha \sinh \alpha \ell\} i_0 / (Z_T + Z_B - 2Z_M). \end{aligned} \tag{A8}$$

Next (A3) is solved for the top conductor voltage, T which yields

$$Z_{in}=T(x=0)/i_0=$$
$$\frac{\{[(Z_BZ_T-Z_M^2)\alpha\ell+(Z_B-Z_M)(Z_M-Z_T)\sinh\alpha\ell]\sinh\alpha\ell-[(Z_M-Z_T)\cosh\alpha\ell-Z_B+Z_M][(Z_B-Z_M)\cosh\alpha\ell+2Z_T-Z_B-Z_M]\}}{(Z_B-2Z_M+Z_T)\alpha\sinh\alpha\ell} \tag{A10a}$$

$$T(x)=\Big\{[Z_T(Z_T-Z_M)+Z_M(Z_B-Z_M)](\ell-x) - (Z_T-Z_M)^2(\sinh\alpha\ell-\sinh\alpha x)/\alpha - (\alpha/y)(Z_T-Z_M)\sinh\alpha x+(Z_T-Z_M) \times[Z_B-Z_M+(Z_T-Z_M)\cosh\alpha\ell] \times\frac{(\cosh\alpha\ell-\cosh\alpha x)}{\sinh\alpha\ell}+(\alpha/y)\Big[Z_B-Z_M + (Z_T-Z_M)\frac{\cosh\alpha\ell}{\alpha\sinh\alpha\ell}\Big]\Big\}i_0/(Z_T+Z_B-2Z_M). \tag{A9}$$

The impedance of this transmission line type structure is shown in (A10a) at the top of the page. If the top and bottom plates are identical (A10a) becomes

$$Z_{in}=[(Z+Z_M)\alpha\ell+2(Z-Z_M)(1+\cosh\alpha\ell)]/(2\alpha\sinh\alpha\ell) \tag{A10b}$$

where $Z=Z_T=Z_B$. When the conductors and dielectric are lossless (A10b) becomes

$$Z_\epsilon=j\Big\{\frac{\omega(L+M)\ell}{2}-\sqrt{\frac{L-M}{2C}} \times\frac{(1+\cos\omega\ell\sqrt{2C(L-M)})}{\sin\omega\ell\sqrt{2C(L-M)}}\Big\}. \tag{A11}$$

From this expression it seems that the characteristic impedance is given by

$$Z_0=\sqrt{\frac{L-M}{2C}} \tag{A12}$$

and the delay time is

$$\tau=\ell\sqrt{2C(L-M)}. \tag{A13}$$

At low frequencies

$$Z_\epsilon=j\Big[\frac{\omega(2L+M)\ell}{3}-\frac{1}{\omega C\ell}\Big] \tag{A14}$$

which is a simple series LC circuit having the dc values of L and C calculable from the geometry and material properties. However, note that the inductance is larger than it would be for an ordinary transmission line equivalent circuit. There it would be $2\ell(L-M)/3$ rather than $\ell(2L+M)/3$. From (A11) the equivalent capacitance $C_{\rm eq}=2C(\sin\Omega/[\Omega(1+\cos\Omega)]$ where Ω is given by

$$\Omega=\omega\ell\sqrt{2C(L-M)}.$$

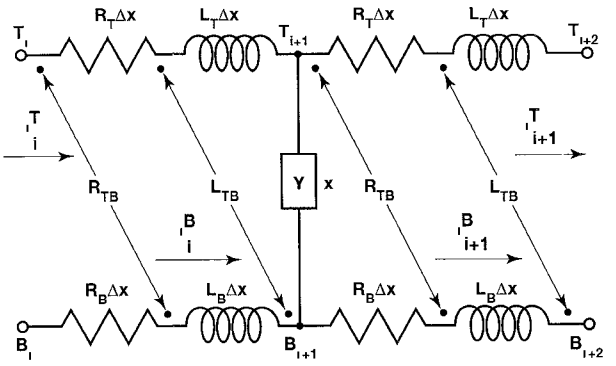

Fig. 13. An element in the circuit of the type B transmission line.

As Ω rises in value $C_{\rm eq}/C$ increases very slowly from unity until $\Omega\to\pi$ where $C_{\rm eq}\to\infty$. For $\pi<\Omega<2\pi, C_{\rm eq}/C$ is negative indicating inductance rather than capacitance. Equation (A6) is set equal to zero and solved numerically by Newton's method of iteration for the Boser and Newsome [2] capacitor. The resulting resonant frequency was 676 megahertz, the same as predicted by ICONSIM in the lossless case.

ACKNOWLEDGMENT

The authors thank W. C. Porter of the Dupont Company for resonant frequency measurements of the capacitor [3], [10] and T. Poulin of Dupont for data on electrode conductivity [8]. We also thank O. Boser of Phillips-North America for discussions concerning his capacitor [2], [6], [10].

REFERENCES

[1] A. T. Murphy, F. J. Young, H. Vandegriff, and J. Curilla, "ICONSIM-computer aided interconnection simulation," in *Proc. 7th Int. EMC Symp.*, Zurich, Switzerland, 1987.
[2] O. Boser and V. Newsome, "High frequency behavior of ceramic multilayer capacitors," *IEEE Trans. Comp. Hybrids, Manufact. Tech.*, vol. CHMT-10, pp. 437–439, 1987
[3] I. Burn and W. C. Porter, "MLC's with copper electrodes for high frequency applications," in *40th IEEE ECTC*, vol. 1, pp. 277–283.
[4] V. F. Perna, Jr., *The RF Capacitor Handbook*, American Technical Ceramics, Division of Phase Industries, Inc., 1979.
[5] N. Coda and J. A. Selvaggi, "Design considerations for high frequency ceramic chip capacitors," *IEEE Trans. Parts, Hybrids Packaging*, vol. 12, no. 3, pp. 206–212, Sept. 1976.
[6] O. Boser, Philips—North America, private communication.
[7] O. Boser and V. Newsome, "High frequency ceramic multilayer capacitor," Philips Lab. Rep, Briarcliff Manor, NY.
[8] T. Poulin, Dupont Electronics, Personal Communication.
[9] S. Matsushita and T. Moto-Oka, "Magnitude of cross-coupling noise in digital multiwire transmission lines," *IEEE Trans. Computers*, C-23, pp. 1122–1132, 1974.
[10] W. Porter, Dupont Electronics, private communication.
[11] D. Moline, "Accurately modeling shunt capacitors," *Microwaves and RF*, pp. 107–109, Feb. 1994.
[12] A. T. Murphy and F. J. Young, "High frequency performance of capacitors," in *IEEE 41st ECTC Proc.*, Atlanta, May 1991, pp. 335–344.
[13] ——, "High frequency design and performance of tubular capacitors," *IEEE Trans. Comp. Hybrids, Manufact. Tech.*, vol. 16, no. 2, pp. 228–237, Mar. 1993.

Arthur T. Murphy (S'49–M'54–SM'61–F'91) received the B.E.E. from Syracuse University and the Ph.D. and M.S. degrees in electrical engineering from Carnegie-Mellon University.

He is a Du Pont Fellow with E.I. Du Pont de Nemours and Co. Inc. He recently completed three years in Japan on assignment from Du Pont as a Visiting Research Fellow. He worked two years at the Sony Research Center in Yokohama, Japan where he developed packaging for high speed GaAs integrated circuits. He spent one year at the International Superconductivity Technology Center in Tokyo, Japan where he developed an active superconducting mixer antenna array. Previously at Du Pont, he established Electronic Systems Research with emphasis on Computer Aided Design of Interconnections called ICONSIM(sm) for Interconnection Simulation. He has also developed a unique UHF filter for control of electromagnetic interference (EMI). He is the co-author of a book, *Introduction to System Dynamics*. Previous to joining DuPont in 1979, he was Brown Professor and Head of Mechanical Engineering at Carnegie-Mellon University and has previously held positions of Vice-President and Dean of Engineering at Widener University, Head of Electrical Engineering at Wichita State University, and Visiting Professor at MIT and University of Manchester (England) and Adjunct Lecturer at Penn State University.

Dr. Murphy is a Fellow of the IEEE and AAAS.

Frederick J. Young received the Ph.D., the M.S., and the B.S. degrees from the Carnegie Institute of Technology.

He is a Consultant in electrical phenomena and magnetohydrodynamics. He was Professor of electrical engineering at the Carnegie-Mellon University for many years and served as the Chairman of the Graduate School of Applied Space Science. He served as Visiting or Adjunct Professor at the University of Tennessee and the Pennsylvania State University. He is the coauthor of the books, *Electromagnetodynamics of Fluids* and *Electrical Engineering Problems*, numerous patents and more than one hundred technical papers.

Dr. Young received the "Young American Electrical Engineer" award of Eta Kappa Nu in 1963.